CrystEngComm

Accepted Manuscript

ROYAL SOCIETY OF CHEMISTRY

www.rsc.org/crystengcomm

Cite this: DOI: 10.1039/c0xx00000x

www.rsc.org/xxxxxx

ARTICLE TYPE

A series of homonuclear lanthanide coordination polymers based on fluorescent conjugated ligand: syntheses, luminescence and sensor for pollutant chromate anion †

Xun Feng,[a,] Rongfang Li,[a] Liya Wang*[a, b], Seik Weng Ng[c,d], Guozhan Qin[a], Lufang Ma [a]

Received (in XXX, XXX) Xth XXXXXXXXX 2015, Accepted Xth XXXXXXXXX 2015
First published on the web Xth XXXXXXXXX 2015
DOI: 10.1039/b000000x

A family of six new homo-lanthanide coordination polymers incorporating conjugated ligand of 2,5-di(2',4'-dicarboxylpheny) pyridine, namely, $\{[Ce(\mu_3\text{-}ddpp)]\cdot 4H_2O\}_n$ (**1**), $\{[Nd(\mu_3\text{-}ddpp)]\cdot 2H_2O\}_n$ (**2**), $\{[Sm(\mu_6\text{-}ddpp)]\cdot H_2O\}\cdot H_2O\}_n$ (**3**), $\{[Eu(\mu_6\text{-}ddpp)]\cdot H_2O\}_n$ (**4**), $\{[Tb(\mu_6\text{-}ddpp)]\cdot H_2O\}_n$ (**5**), $\{[Er(\mu_6\text{-}ddpp)]\cdot H_2O\}_n$ (**6**), (H_3ddpp = 2, 5-di(2',4'-dicarboxylpheny) pyridine acid, have been prepared successfully through solvothermal reactions. The polymers **1–6** exhibit various coordination environments and different multi-dimensions, but they all are assembled in one dimensional (1-D) Ln-carboxylate chain. Polymer **1** just shows 1-D ribbon chain, while polymer **2** exhibits binodal (3, 8)-connected topology net. Heavy lanthanide polymers **4-6** possesses 3D frameworks based on a rare (4, 8)-connected **msw** framework. Thermogravimetric and different thermal analysis measurements indicate that they all display high thermal stability. The luminescence emission spectra display characteristic *f-f* transition emissions of Ln(III) polymers in visible or near infrared (NIR) regions. The fluorescent ligand H_2ddpp provides efficient energy transferring for the sensitization of Eu(III) and Tb(III) ions in visible region, among which Tb(III) polymer may be employed as fluorescence ratiometric probe for pollutant CrO_4^{2-} anion.

.

Introduction

Lanthanide coordination polymers (LnCPs) or lanthanide organic frameworks (LnOFs) have been at the forefront of inorganic chemistry and materials fields for a long time, because of their special chemical and physical properties arising from the unique spectroscopic and 4*f* electronic orbital being shielded by the $5s^2$ and $5p^6$ shells. Lanthanide luminescence is a very attractive tool particularly for biological imaging and luminescence sensing,[1] resulting in their potential applications as electroluminescent devices, MRI imaging agents or bioprobes for immunoassays.[2] In fact, such applications became possible thanks to lanthanide ions exhibiting pure, long-lived and narrow emission bands, and can emit luminescence ranging from visible regions (Eu(III), Tb(III)) to near infrared Near- infrared (NIR) luminescence (Pr(III), Nd(III), Er(III)), which is currently attracting considerable interesting in the fields such as optical communication, and biological assays etc.[2] However, in the case of the lanthanide-based fluorescence, one common strategy to overcome the problem of the Laporte forbidden *f–f* transitions is to use conjugated organic ligands as chromophores in order to ensure an efficiently energy transfer to the lanthanide ion.[3] Luminescence from lanthanides is usually sensitized by excitation of strongly absorbing organic ligands bound directly to the lanthanide centers through an antenna effect.[4] Usually, the presence of anion aromatic organic system affords the fully allowed π–p*, π–π* transitions, thus leading to a possible effect energy transferring.[5,6] Our strategy to incorporate the pyridine units substituted with aromatic chelating system into the Ln(III) polymer, which is available to enlarge the conjugated structure and enhance absorption. The chelating luminescent ligands can encapsulate and link Ln(III) ions to form polynuclear compound or polymer.[7, 8] In addition, chromate (CrO_4^{2-}), toxic anion can be accumulated in living organisms leading to cancer, deformity and gene mutation.[8] It severely harms human health and environments. However, it has been still seldom reported for detection these pollutant small ions using the reusable and retailored MOFs. In this contribution, the combined biphenyl tetracarboxylic acid with pyridine as the new kind of organic ligand with introduction an extended π-conjugated system, 2, 5-di(2',4'- dicarboxylphenyl) pyridine (ddpp) has been employed, which can acts as a multi-donor linker for construction of coordination polymers with potentially interesting properties.[9] The introduction the electron

donating species (*e g*, benzene group) to aromatic acid is expected to enhance the coordination ability of ligand and facilitate the electron transferring within these compounds. As a continuation of our previous investigations,[10] new family of lanthanide-organic polymers have been isolated successfully and been characterized, among which framework **5** can be used as potential luminescent probe for toxic anion.

Experimental section

Materials and methods

The ligand H_3ddpp was synthesized similarly as described in the literature procedure,[10] with help of Jinan Camolai Trading Company of China and other reagents were obtained commercially and used without further purification. The IR spectra were recorded as KBr pellets on a Nicolet Avatar-360 spectrometer in the range of 4000 to 400 cm^{-1}. Thermogravimetric analysis (TG) is carried out on a SDTQ600 thermogravimetric analyzer. A platinum pan was used for heating the sample with a heating rate of 10 °C/min under nitrogen atmosphere. Fluorescence measurements were recorded with Hitachi F4600 fluorescence spectrophotometer. All reagents used in the syntheses were of analytical grade and used as received. Elemental analyses for carbon, hydrogen and nitrogen atoms were performed on a Vario EL III elemental analyzer. The infrared spectra (4000-400 cm^{-1}) were recorded by using KBr pellet on an Avatar TM 360 E. S. P. IR spectrometer. The powder X-ray diffraction (PXRD) patterns were measured using a Bruker D8 Advance powder diffractometer at 40 kV, 40 mA for Cu Kα radiation (λ = 1.5418 Å), with a scan speed of 0.2 s/step and a step size of 0.02 (2θ). Luminescence spectra of the complexes in solid state were carried out on a Cary Eclipse fluorescence spectrophotometer. Solid state luminescence spectra in the near-Infrared region were measured at room temperature with an Edinburgh instrument FLS920 fluorescence spectrometer.

Syntheses of series of lanthanide compounds

The same procedure was employed in preparation the polymers **1**-**6**, hence, polymer **1** will be described in details herein. A mixture of $Ce(NO_3)_3.6H_2O$ (0.044 g, 0.1 mmol) for **1** and $(Sm(NO_3)_3{\cdot}6H_2O$, 0.0435 g for (**2**), $Eu(NO_3)_3{\cdot}6H_2O$, 0.044 g for (**3**), $Gd(NO_3)_3{\cdot}6H_2O$, 0.0455 g for (**4**), $Tb(NO_3)_3{\cdot}5H_2O$, 0.043 g for (**5**), and $Er(NO_3)_3{\cdot}5H_2O$, 0.044 g for (**6**) were mixed with an aqueous NaOH solution (including 5 ml ethanol) of H_2ddpp (0.042, 0.1 mmol). After stirring for 20 min in air, and the pH value was adjusted to 5.5. The mixture was placed into 25 mL Teflon-lined autoclave under autogenous pressure being heated at 140 ^{o}C for 72 h, and then the autoclave was cooled over a period of 24 h at a rate 5 ^{o}C/h. The colourless crystals of **1** were obtained in yield: 0.0232 g (41%) (based on lanthanide element, the same below). Elemental analysis (%): calcd. for $C_{21}H_{18}CeNO_{12}$: C 40.92, H 2.94, N 2.27, found: C 40.59, H 2.76, N 2.43. IR (KBr pellet, cm^{-1}): 3432s, 3122br, 2253s, 1623s, 1532s, 1413m, 1374s, 747m, 668s, 457m. For **2**, yield): 0.0144 g (34%). Elemental analysis Anal calcd for $C_{21}H_{12}NO_9Nd$: C 44.52, H 2.13, N 2.47, found: C 44.29, H 2.21, N 2.29. IR: 3420vs, 2066s, 1784s, 1626vs, 1442s, 1392s, 1012vs, 910s, 832s, 723s. For **3**, yield: 0.0214 g (41%). calcd. for $C_{21}H_{15}NO_{10.5}Sm$: C 42.06, H 2.52, N 2.35, found: C 42.20, H 2.49, N 2.33. IR: 3234br, 1661s, 1427s, 1394s, 1013m, 780s, 652m. For **4**, yield: 0.0216 g (38%). Elemental analysis (%): calcd for $C_{21}H_{12}EuNO_9$: C 43.91, H, 2.11, N 2.43, found: C 43.85, H 2.21, N 2.41. IR: 3420vs, 2256s, 1626vs, 1612s 1442s, 1392s, 1319m, 1179m, 1012vs, 832s, 810m, 663s. For **5**, yield: 0.0167 g (37%). Elemental analysis (%): calcd for $C_{21}H_7TbNO_8$: C 45.04, H, 1.26, N 2.50, found: C 44.85, H 1.27, N 2.53. IR: 3420vs, 2163s, 1618s 1439s, 1392s, 1279s, 882s, 810m, 693s. For **6**, yield: 0.0170 g (39%). Elemental analysis (%): calcd for $C_{21}H_{12}NO_9Er$: C 42.78, H 2.38, N 2.37, found: C 42.79, H 2.41, N 2.38. IR: 3441m, 3286br, 1609s, 1528s, 1427s, 1410m, 1337s, 1075m, 835s, 783vs, 660s.

X-ray crystallographic data collection and refinement

Single-crystal diffraction data of polymers **1–6** were collected on a Bruker SMART APEX CCD diffractometer with graphite-monochromated Mo *Kα* radiation (λ = 0.71073 Å) at room temperature. The structures were solved using direct methods and successive Fourier difference synthesis (SHELXS-97),[11(a)] and refined using the full-matrix least-squares method on F^2 with anisotropic thermal parameters for all nonhydrogen atoms (SHELXL-97).[11(b)] An empirical absorption correction was applied using the SADABS program. The hydrogen atoms of organic ligands were placed in calculated positions and refined using a riding on attached atoms with isotropic thermal parameters 1.2 times those of their carrier atoms. The summary crystallographic data, the selected bond lengths and angles, hydrogen bonding parameters for polymers **1–6** are listed in Table 1, S1 and S2, ESI †, respectively.

Results and discussion

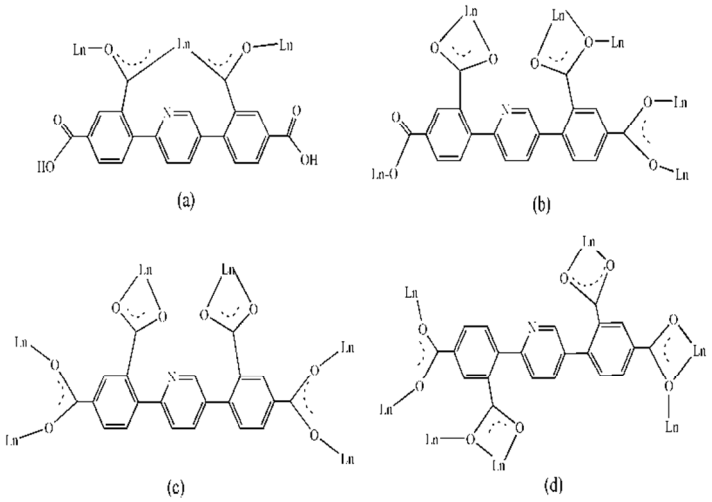

Scheme 1. Illustration of the lanthanide clusters aggregate linked by H_3ddpp ligand in the series of polymers.

Table 1. Crystal data and structure refinements for polymers 1-6

Empirical formula	$C_{21}H_{18}NO_{12}Ce$ (**1**)	$C_{21}H_{12}N\ O_9Nd$(**2**)	$C_{21}H_{15}NO_{10.5}Sm$ (**3**)	$C_{21}H_{12}NO_9Eu$(**4**)	$C_{21}H_7NO_8Tb$(**5**)	$C_{21}H_{12}NO_9E\ r$ (**6**)
Formula weight	616.48	566.56	599.69	574.28	560.20	589.58
Temperature (K)	293(2) K	293(2) K	293(2) K	293(2) K	296(2) K	293(2) K
Wavelength (Å)	0.71073	0.71073	0.71073	0.71073	0.71073	0.71073
Crystal system	Monoclinic	Triclinic	Triclinic	Monoclinic,	Monoclinic	Monoclinic
Space group	C2/c	P-1	P -1	C2/c	C2/c	C2/c
Unit cell dimensions (Å, °)	a = 14.7932(12) b = 14.7382(11) c = 10.6919(8) β= 112.2890(10)	a = 9.3219(6) b = 10.5274(6) c = 11.1369(7) α= 64.340(1) β= 80.881(1) γ= 82.009(1)	a=9.4281(6) b=10.5623(7) c=11.1893(7) α= 64.0602(9) β= 80.8746(9) γ= 82.0709(8)	a = 18.3160(14) b = 12.2002(9) c = 9.5032(7) β= 114.0860(10)	a = 17.72(4) b = 12.11(2) c = 9.324(19) β= 113.41(3)	a = 18.3160(14) b =12.2002(9) c =9.5032(7) β=114.0860(10)
Volume ($Å^3$), Z	2156.9(3), 4	969.64(10)	986.36(11), 2	1938.7(3), 4	1836(6), 4	1938.7(3), 4
D_{caled}, (g/cm^3)	1.898	1.940	2.019	1.968	2.027	2.020
Absorption coefficient (mm^{-1})	2.181	2.735	3.044	3.293	3.905	4.387
F(000)	1220	554	588	1120	1076	1140
θ Range for data collection (°)	2.03- 27.49	2.04- 27.50	2.15- 27.50	2.07 - 27.50	2.51- 25.48	2.07- 27.50
Independent reflections	2456	4248	4374	2208	1653	2208
Observed reflections	6258	5663	6073	5806	3737	5806
Refinement method	Full-matrix least-squares on F2	Full-matrix least-squares on F2	Full-matrix least-squares on F2	Full-matrix least-squares on F2	Full-matrix least-squares on F2	Full-matrix least-squares on F2
Data/restraints/parameters	2456 / 1/ 159	4248 / 0 / 289	4374 / 15 / 318	2208 / 96 / 150	1653 / 38 / 141	2208 / 96 / 150
Goodness-of-fit on F^2	1.035	1.096	1.042	1.133	1.017	1.108
R index (I > 2σ(I))	R1 = 0.0308 wR2 =0.0741	R1 = 0.0353 wR2 = 0.0941	R1 = 0.0240 wR2 = 0.0589	R1 = 0.0298 wR2 =0.0854	R1 = 0.0812 wR2 = 0.1582	R1 = 0.0374 wR2 = 0.1113
R index (all data)	R1 = 0.0358 wR2 = 0.0780	R1 = 0.0396 wR2 = 0.0966	R1 = 0.0240 wR2 = 0.0589	R1 = 0.0320 wR2 = 0.0870	R1 = 0.1249 wR2 = 0.1752	R1 =0.0399 wR2 = 0.1135
Largest diff. peak/ hole ($eÅ^{-3}$)	0.936 / -0.744	2.322 / -2.280	1.135 / -1.094	1.096 /-0.764	1.492/ -2.169	1.552/ -0.708

. $R=[\sum||F_0|-|F_c||/\sum|F_0|],\ R_W=\sum_W[|F_0^2-Fc^2|^2/\sum_W(|F_w|^2)^2]^{1/2}$

IR spectra

In the IR spectra of compounds **1-6**, the presence of the broad and strong stretches in frequency region of 3200-3450 cm^{-1} are assigned to the characteristic peaks of -OH vibration of free water or -NH vibrations. The strong vibrations appeared around 1580 and 1450 cm^{-1} correspond to the asymmetric $\nu_{as}(COO^-)$ and symmetric stretching $\nu_s(COO^-)$ vibrations modes of carboxylic groups.[12] The strong absorptions at *ca*. 800 cm^{-1} indicate the existence of 1,3 substituted benzene group. In IR spectra of **1-5**, the absence of strong bands ranging from 1690 to 1710 cm^{-1} indicates that the completely deprotonation of carboxylic groups of aromatic carboxylic tectonic.[13]

Structural descriptions

Single X-ray diffraction analyses reveal that all the compounds are found to be metal coordination polymers, based on binuclear lanthanide-carboxylate aggregates. They are all crystallizing in monoclinic system, with space group of C2/c except Nd(III) and Sm(III) complexes crystallizing in triclinic system, with space group of P_{-1}. Therefore, structure of **1** was selected and described in details to represent. As illustrated in Fig. 1(a), the asymmetric unit of **1** is a neutral mononuclear cerium polymer. It contains an eight-coordinated Ce(III) ion, one Hddpp anion ligand, and two coordinated water molecule. For H_3ddpp, one of the carboxylic groups has been deprotonated, while another H atom was added to pyridine N resulting in the zwitterion species. The coordination sites were occupied by oxygen atom from water molecules or carboxylates. Eight bonds with different lengths give rise to a distorted dodecahedral environment around the Ce(III) ion. All

the distances of Ce-O vary from 2.419(3) to 2.636(3) Å, which are closely similar to those observed in several related species.[14] All Hddpp anion ligands have the same coordination mode in a bridging manner, employing carboxylic group doubly connecting two Ce(III) ions to form a binuclear unit with the shortest the separation Ce···Ce of 5.40 Å, resulting in an eight memembered chair-like ring. The binuclear Ce_2 aggregates lies in a C_2 center position of [Ce(ddpp)] architecture, (Scheme 1a). The dihedral angle between the neighbouring benzene rings sharing the common Ce_2 dimer is just 0°. Interestingly, the pyridine-N does not coordinate to central ion. The ubiquitous bridging ligand H_3ddpp also connects the two adjacent binuclear units *via* its' carboxylate oxygen atoms in a μ_2-η^1:η^1 fashion, propagating these eight membered rings and giving rise to a 1D infinite ribbon zigzag chain array along the crystallographic *c* axis, as displayed in Fig 1(b). Hydrogen bonding interactions further interlink these 1D chains into 2D corrugated netlike sheet. Moreover, the 2D layers are assembled into a 3D framework *via* hydrogen bonding interaction from the free water molecules and coordinated water molecules, and from the coordinating carboxylate oxygen atoms and the free water molecules, as shown in Fig. S1, ESI †.

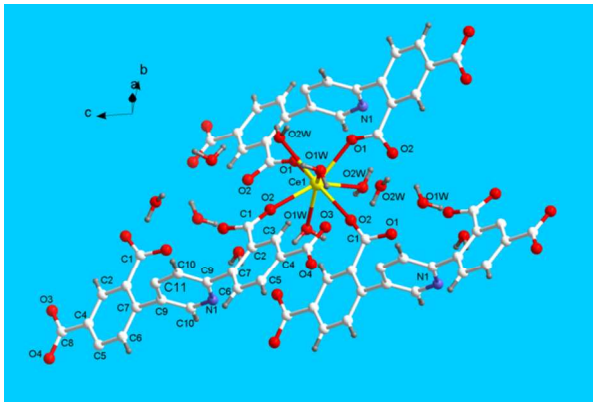

(a)

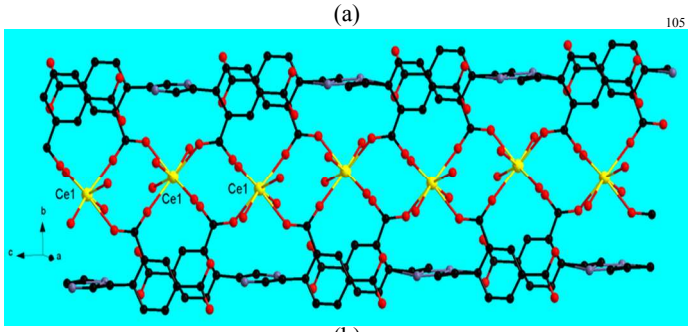

(b)

Fig. 1 (a) The coordination environment of Ce(III) cation in **1** viewed along *a b* plane. (b) Ball and stick diagram of the 1D alternative chain in polymer **1.** Free water molecules have been omitted for clarity

As depicted in Fig. 2(a), Nd(III) polymer **2** has slightly different coordination modes and unit structure as **1**. In **2**, ddpp links four adjacent Nd(III) ions, in which carboxylic group chelate the Nd (III) ions, while the 4- carboxylate atom (O2) employs an μ_2-O bidentate coordination mode to bridge two adjacent Nd(III) ions, resulting in a binuclear Nd (III) unit based on paddle-wheel subunit rather than simple carboxylic-linked binuclear unit with the separation of Nd···Nd of 5.330 Å, as shown in Fig. S2, ESI †. Carboxylic group from isophthalate moiety extends the binuclear units into 1D double chain polymer. (See Scheme 1b). The binuclear units are connected alternatively by carboxylic oxygen atoms (O5, O6) of Hddpp ligands to form the 1D linear chain along the *b* axis (Fig. 2(b)). The infinite 1D chain extends to a 2D layer in the *bc* plane, and then these units are further propagated into 3D framework along ab plane Fig. 2(c).

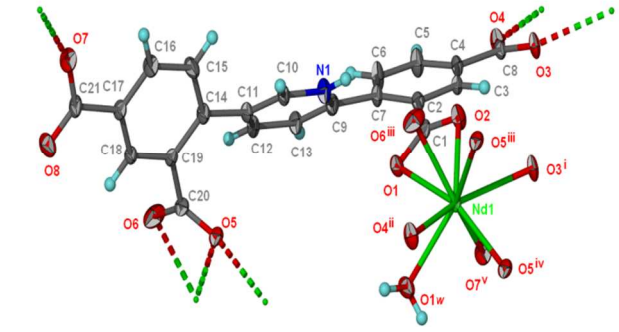

(a)

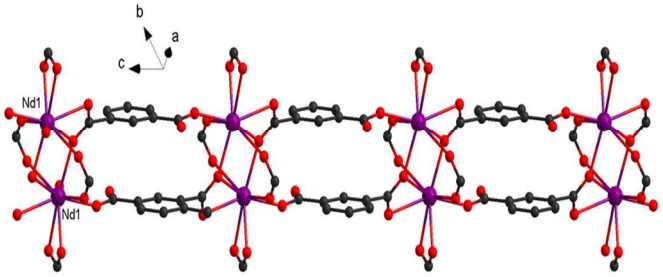

(b)

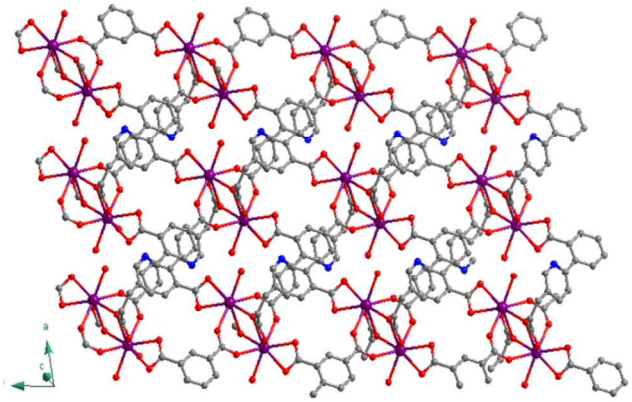

(c)

Fig. 2 (a) the coordination environment of Nd(III) in **2**. (b) Diamond illustration of the 1D double chain connected by carboxylic oxygen in **2** along *c* axis. (c) Projective view of 2-D corrugated layer consisting of 1D double chain along *a b* plane. Nd(III) ion is presented by the pink ball. The H atoms and free waters are not included for clarity.

The method used for topological analysis follows a recent review. The tetratopic organic linkers are simplified as two linked triangles in this case. The identification of the nets is performed through the program *Systre* [15] and the database *RCSR*.[16] In Nd(III) polymer **2**, the secondary building unit (SBU) is a binuclear Nd(III) cluster, which has eight points of extension and

therefore can be simplified as an 8-connected node (Fig.3).[17] By counting the two 3-connected nodes of the linker, the overall framework can be topologically regarded as a binodal $(3\text{-c})_4(8\text{-c})$ net with the point symbol 3 of $(4.6^2)_4(4^4.6^8.8^{12}.10^4)$, identified by the program *TOPOS*.[18] The net shown in Fig. 3 (down) is the augmented form of this (3, 8)-c net.

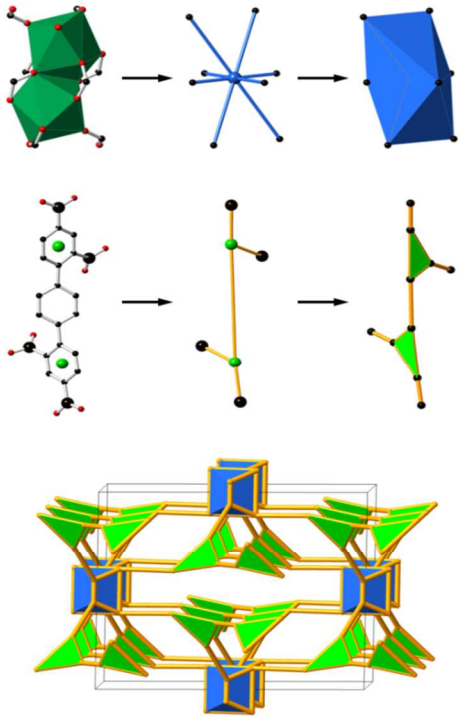

Fig 3. Topological analysis of **2** by simplifying the SBU into an 8-c node (up) and the ligand into two linked 3-c nodes (middle), giving a (3, 8)-c net in the augmented form (down).

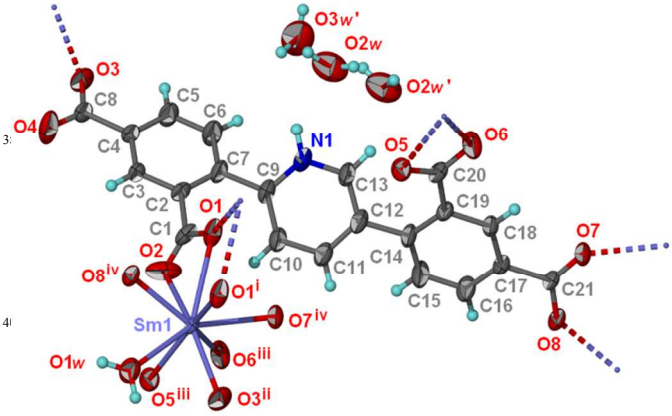

Fig. 4. Coordination environment of Sm(III) ion in **3**. Symmetry codes: # i -x+1,-y,-z+1, #ii x+1, y, z, #iii -x,-y+1,-z+1, #iv x, y, z+1.

For Sm(III) polymer **3**, it is slightly different from previous two polymers. It is an infinite 3D lanthanide organic frame work that crystallizes in triclinic system, space group *P*-1. The asymmetric unit contains Sm(III) atoms, a completely deprotonated H_3ddpp ligands and one coordinated water as well as two uncoordinated water molecules. The coordination polyhedron around the Sm(III) ion can be visualized as a distorted tricapped trigonal prism geometry with a $[SmO_9]$ donor set (Fig. 4), in which the seven coordination oxygen atoms are from carboxylic groups, as indicated in Fig. S3, ESI †. The remaining two sites were occupied by oxygen atom of water molecules, completing the nine–coordination configuration. The ddpp ligand employing bridge mono dentate and chelate μ_6-(η^2: η^2:η^1: η^1)-O fashions to ligate six Sm (III) ions. One carboxylic group connects adjacent Sm(III) ions into a dimer unit. Alternatively speaking, the ddpp ligand employs the 2'-carboxylate group to chelate the central Sm(III) ion and further to connect the adjacent Sm (III) ion of next unit (see Scheme 1(d)). Therefore two adjacent Sm (III) ions are quadrifold bridged by the carboxylic group and further doubly bridged by carboxylate oxygen atoms from isophthalate moiety into a centrosymmetric dimeric unit instead of the paddlewheel arrangement with the Sm···Sm distance of 4.089 Å, followed by 4-carboxylate group intercrossing these units. These units are further into a grid sheet, as shown in Fig 5(a). In this sheet, adjacent Sm(III) ions were alternatively connected by two carboxylates from Hddpp to form a 1D chain composed of eight-membered ring, as shown in Fig. S4, ESI †, which is neither similar to other reported transition metal polymers, in which the central ions are connected through ambient ligands to form honeycomb homometallic layers,[19] nor it is different from the lanthanide polymers containing isonicotinic acid tectonic and oxalate coligand.[20] However, when the binuclear Sm_2 unit doubly connected *via* carboxylic group is regarded as a four connected node, the whole structure can be described as a uninodal 4-connected corrugated network, with 4,4 **sql** topology.[21] The point symbol is 6^3, and the 3D packing diagram of **3** is shown in Fig. 5(b).

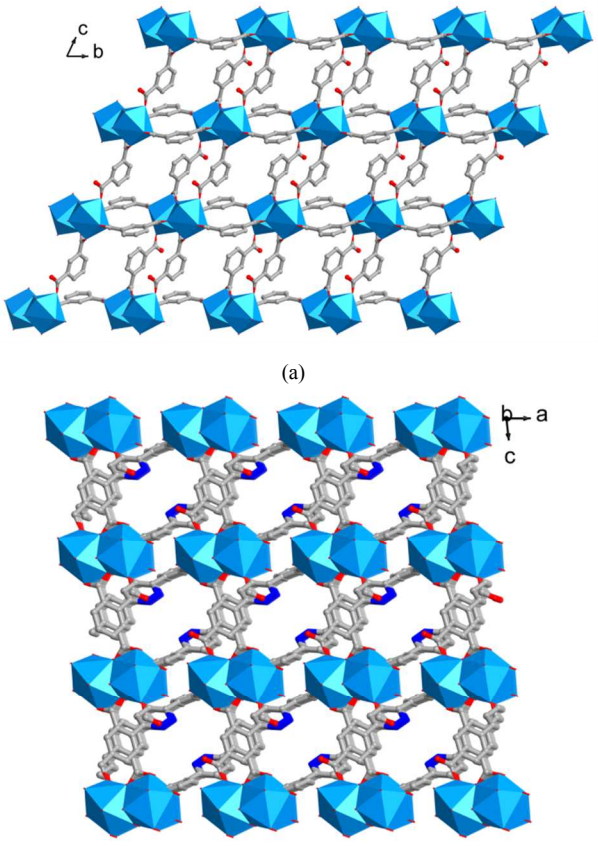

(b)

Fig 5. (a) Perspective view of 2-fold stacking 2D net with a **sql** topology of **3**. (b) The 3D framework of **3** formed by the parallel stacking of the 2D layers. Hydrogen atoms are omitted for clarity.

In contrasting with 2D polymers of **2**, **3**, the **4-6** possess 3D framework. They display similar arrangement, and the Eu(III) polymer **4** is employed to descript their structures. In **4**, the centrosymmetry unit is composed of one dpp ligand and two Eu(III) ions. The ddpp ligand adopts an interesting bridging coordination mode, namely, μ_6-kO, O :k O',O′: k O″,O″ to simultaneously connect six Eu(III) ions in bis- monodentate chelating and bridging monodentate fashions, as illustrated in Scheme 1c and Fig. S5(a) and S6, ESI, †. The central Eu (III) is surrounded by eight oxygen atoms forming a near perfect square anti-prism local symmetry. 4- carboxylate oxygen connects adjacent Eu(III) ions into binuclear units, followed by the binuclear units being further extended into 1D robust chain. As shown in Fig. S5(b), ESI, †. This coordination is essentially not comparable to octa- and nona-nuclear clusters with β-diketonate ligands, and 3D lanthanide framework containing aromatic carboxylate ligand, already described.[22]

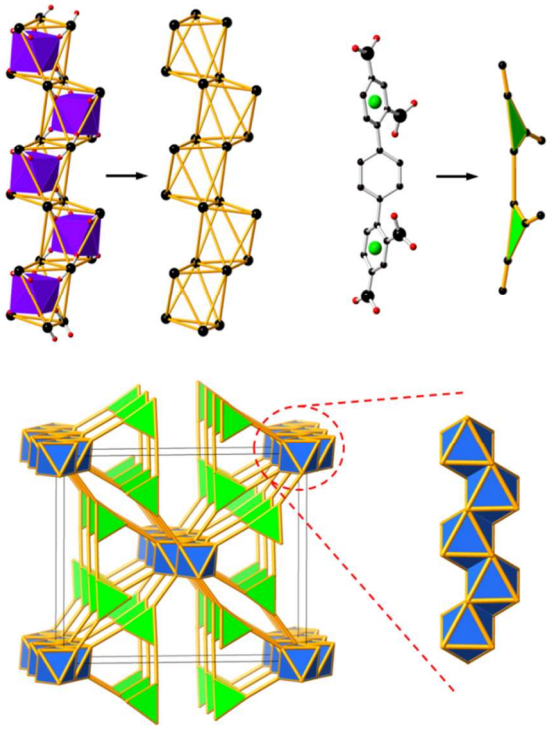

Fig.6. Schematic representation of the **MSW** topology in **4** with different nodes discriminated by colours.

As illustrated in Fig.6, topological analysis of Eu(III) polymer can by simplifying the rod SBU into a column of edge-sharing octahedra (up left) and the ligand into two linked triangles (up right), giving a rod net in the augmented form (down). In polymer **4**, the SBU is an infinite 1D EuO_8 chain, known as rod SBU,[23] which is different from the type in Nd(III) and Sm(III) polymers. The shape of the rod SBU in **4** is found to be rare edge-sharing octahedron, similar to a recent reported one, [24] which is different from the more usual face-sharing octahedral rod SBU. The Hddpp ligand is also simplified as two linked triangles.[25] Combining this rod SBU and the two linked triangles, results in the whole point symbol for this net: 6-connnected **msw** network with point symbol of $(4^8.6^7)$, and the underlying topology of **4** is an augmented rod net shown in Fig. 6 (down). Carefully inspection of the structure reveals that these corrugated layers are further stacked together through strong interlayer hydrogen interactions between carboxylic group and free water oxygen atoms from the adjacent 2-D sheets, such as [O···O = 2.765(3) Å, O···H -O = 165.2°], as demonstrated in Fig. S1, ESI †, (for polymer **1**). The hydrogen bonding parameters are listed in Table S2, ESI † for details. It should be pointed out that in present work, the compounds exhibit different coordination polymer arrangement from the light rare earth cerium polymer of **1** to the heavy rare earth erbium compound of **6**. Ce(III) polymer **1** is just 1D ribbon chain, Nd(III) and Sm(III) polymers exhibit 2-D corrugated lamellar, while Eu(III), Tb(III), Er(III) polymers construct 3D frameworks. This case is also similar to those of other reported series lanthanide coordination compounds with diverse structures based on the multi-N, O-donor ligands.[4a,6b, 23b] However, for light or heavy family lanthanide polymers, similarities in bonding motifs for the series of lanthanide complexes allow us to compare the metal-ligand distances in the same array. The average Ln-O distances have been listed in Table S1, ESI, †. As the ionic radius of the lanthanide center become smaller in the order of Nd(III) > Sm(III)> Eu(III)> Tb(III)>Er(III), their corresponding average bond lengths decrease slowly, consistent with the so-called lanthanide contraction effect. In addition, Ln(1)···Ln(1) separation bridged by carboxylate could only be compared for polymers that exhibit the same array, these metal···metal separations comparative investigation on the isostructural polymers **2-3**, and **4-6** have found that in same 1-D chain, the Ln(1)···Ln(1) separation also display their slightly decreasing trend with increasing of elements order, which are also in accordance with the ''lanthanide contraction'' effect [26].

Table 2. Comparing Ln···Ln metal separations for series of polymers

Polymers **2-3**	Separation (Å)	Polymers **4-6**	Separation (Å)
Ce(1)···Ce (1)	4.089	Eu(1)···Eu (1)	5.772
Sm(1)···Sm (1)	4.073	Tb(1)···Tb (1)	5.655
		Er(1)···Er (1)	5.620

PXRD measurements and thermal analysis

The purities and crystallinities of the bulk products of **1-6** were determined by comparison of the simulated and experimental X-ray powder diffraction patterns, and the results are reported in Fig. S7, ESI †. The peak positions of the experimental patterns are nearly matched with the corresponding simulated ones generated from single crystal X-ray diffraction data, although some minor Bragg peak positions have been shifted in comparison to the simulated ones. The thermal stability of **1–6** was also explored by thermogravimetric analysis (TG). The results are reported in Fig. S8, ESI †, from which we can see compounds **1–6** exhibit the nearly similar thermal trend. So, here the compound **1** is used to as a representative. The TGA trace of

1 exhibits an initial mass loss of 12% corresponding to remove initially of one guest water as well as two coordinated water molecules in the temperature about 220 °C, and the decomposition of **1** begins above 250-270 °C, which is attributed to the release of 1 mol carboxylic group 22 % (calcd. 3.38%). The compound **1** begin to decompose following upon further heating and underwent a rapid and significant weight loss of 32.8% beyond the temperature of 450 °C, corresponding to the destruction of the H_2ddpp organic ligands (calcd. 34.1%), the subsequent steps cannot be easily identified and are likely to be a combination of pyridine or benzene carboxylate decomposition. No reasonable fragments can be assigned corresponding to the further weight loss processes beyond 900 °C, possibly due to the compounds being decomposed to Ln_2O_3.[27]

Photo -luminescence properties

Lanthanide compounds have been used to develop several technological applications due to the photoluminescent properties that encompass not only trichromatic fluorescent tubes and multi colour displaying devices but also MRI agent for biomontoring, optical amplifiers, and perhaps metal-organic light-emitting diodes in future.[28] They exhibit characteristic luminescent emissions in the visible to near-infrared part of the optical spectrum, arising from the $4f^n$ electronic configuration, and electronic transitions.[29] The photoluminescence properties of the solid samples of **2**, **3**, **4, 5, 6** and the free H_3ddpp ligand were investigated at room temperature upon photo -excitation, as depicted in Fig.7 to Fig. 10 and Fig. S9 to Fig. S13, ESI, †, respectively. As illustrated in Fig. S10, ESI †, the H_3ddpp ligand exhibits strong solid-state emissions maximum at 408 nm in the edge of visible region at room temperature, which mainly originate from the intraligand $\pi\rightarrow\pi^*$ transitions of H_3ddpp conjugation ligand.

Visible region luminescence of compounds

Under excitation at 328 nm, polymer **3** exhibits the series of characteristic emission band of Sm(III) ion at 548, 597, 653 nm, respectively, see Fig. S11, ESI †, which is attributed to $^4G_{5/2}\rightarrow{}^6H_{5/2}$, $^2P_{5/2}\rightarrow{}^8S_0$, $^4G_{5/2}\rightarrow{}^6H_{7/2}$ transitions for the Sm(III) ion. The highest intense red fluorescent emission band at λ_{max} = 548 nm. It is remarkable that the lowest triplet state energy of H_3ddpp is 408 nm, and is higher rather than be comparable to the energy of ground state of Sm(III), $^5G_{5/2,}$ which his 562 nm. It cannot sensitize Sm (III) fluorescence efficiently, according to Dexter theory.[30] The emission band profile maximum at 388 of Sm(III) is similar to the ones of free H_3dppp ligand, maybe the triplet state of this ligand is significantly blue-shifted in this case. This is due to the presence of two aromatic-substituents, which is required for the coordination of the lanthanide cations. This also indicates that the energy absorption of the triplet state of the ligand can transfer partial energy from ligand to Sm (III) ion.[31] The emission spectra of **3** also show a major peak at 435 nm, presumably assignable to the ligand-to-metal energy transfer. With respect to the emission of the pure H_3ddpp ligand, the enhancement of intensity and the small red shift of the emission of Sm-ddpp may be attributable to the increase of rigidity of H_3dppp ligand upon coordination with the metal ion, helping to reduce the loss of energy otherwise occurring *via* radiationless decay of the intraligand emission excited state.[32] As reported in Fig. 7, upon excitation at 345 nm compound **4** displays series intense luminescence with two emission bands occurring at 556, 594, 616, 702 nm that can be assigned to $^5D_0\rightarrow{}^7F_J$ transitions (J = 1, 2 and 3, respectively).[33] The $^5D_0\rightarrow{}^7F_2$ and $^5D_0\rightarrow{}^7F_1$ transitions are electronic dipole and magnetic dipole, respectively, which makes the former (known as hypersensitivity) to be extremely sensitive to site symmetry, whereas the latter is mainly sensitive to the magnetic dipole effect created by the crystal field environment and is practically not influenced by the chemical surrounding of the Eu(III) ion. The intensity of the $^5D_0\rightarrow{}^7F_2$ transition, which is responsible for brilliant red emission of the compound, is about three times stronger than that of the $^5D_0\rightarrow{}^7F_1$ band, indicating that the Eu(III) ion occupies low-symmetry sites without inversion center, in agreement with the structural analyses above mentioned. It is noteworthy that the Eu(III) polymer shows a higher intense fluorescence emission than that of the free N- heterocyclic dicarboxylic acid ligand.[34] It is remarkable that the emission profile of H_3ddpp ligand does not present in emissions inclusion of trivalent Eu(III) cations, indicating complete energy transfer from the ddpp ligand to the Eu(III) ion, so-called antenna-effect, as displayed in Fig.7, as it happens usually,[35] indicates energy transfer from this triplet excited state to the lanthanide ion. The presence of the $^5D_0\rightarrow{}^7F_0$ transition, the fine structure of the $^5D_0\rightarrow{}^7F_{1-4}$ transitions, and a large value of the intensity ratio $R = I(^5D_0\rightarrow{}^7F_2)/I(^5D_0\rightarrow{}^7F_1)$ are consistent with the low-symmetry coordination environment.[36, 37]

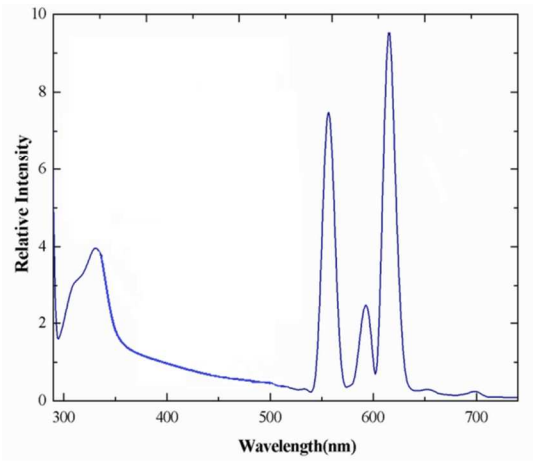

Fig. 7 Room-temperature emission spectra for compound **4** monitored approximately at 328 nm excitation in the solid state.

Regarding the terbium polymer **5**, it emits green dominated luminescence upon excitation at 358 nm with the emission bands peaking at 486, 543, 581, 627 and 653 nm, as reported in Fig. S12, ESI †. These are originated from the characteristic $^5D_4\rightarrow{}^7F_J$ transitions (J = 6, 5, 4, 3 and 2).[38, 39] The typical green emission is observed for the polymer **5**, dominated by the $^5D_4\rightarrow{}^7F_5$ transition (545 nm), together with additional peaks at 488 nm ($^5D_4\rightarrow{}^7F_6$), 585 ($^5D_4\rightarrow{}^7F_4$) and 620 nm ($^5D_4\rightarrow{}^7F_3$). Nonetheless, the polymers' stability prevents the coordination of water molecules in the first coordination sphere and resulting concentration quenching, leading to very efficient luminescence in aqueous solution. The fluorescence quantum yields of Eu(III) and Tb(III)

fluorescence (Y_{Ln}) have been estimated by reference method using quinine sulfate as standard sample according to equation as following: $Y_{Ln} = Y_s.F_u/F_s.A_s/A_u$, where Y_{Ln} and Y_s represent the test Ln(III) compound and reference material fluorescence quantum yield, respectively. A_u and A_s represent absorption intensity of the test substance and reference substance. F_u and F_s represent the fluorescence intensity integration of the test substance and reference materials, correspondingly. It gives values of 13.14% and 15.1% for polymers **4** and **5**, respectively.

To explore the effect of CrO_4^{2-} on the luminescence of **5**, liquid-state photoluminescent (PL) spectra were investigated in $NH_3.H_2O$ –NH_4Cl buffered aqueous solution (pH =7.4). Upon titration with K_2CrO_4 solution in dimethylformamide (DMF), the emission intensity changes upon variation of added K_2CrO_4 solution (2 mol/L) are demonstrated in Fig. 8. The addition solution of K_2CrO_4 to buffered solution of **5** caused significant changes in emission spectra. With one drop of K_2CrO_4 solution was added, the typical luminescence peaks of Tb(III) are still in occur obviously at 492 and 547 nm, respectively. As CrO_4^{2} continuously interaction with polymer **5**, the luminescent intensity dropped rapidly. Titration of **5** with K_2CrO_4 solution in gives complete quenching of the luminescence 8 equiv. of K_2CrO_4 was added. This is also probably due to the Hddpp ligand coordination to Cr(VI) centre decreasing the conformational rigidity of the aromatic ligand, thereby enhancing the non-radiative decay of the intraligand (π–π*) excited state.[40] The function diagram representing fluorescence intensity verse concentration of K_2CrO_4 added is displayed in Fig. S13, ESI, †. After the samples were immersed in for 12 hours, the PXRD patterns keep intact as in Fig. S14, ESI, †, which indicates the frameworks materials are stable in this conditions. Thus, polymer **5** may be considered as luminescent probe of CrO_4^{2-}, which has been seldom reported as a MOFs materials application hitherto.[38]

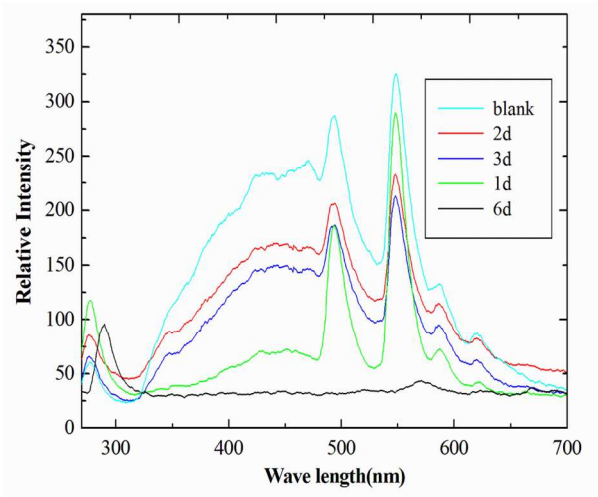

Fig. 8 Emission spectra of polymer **5** in buffered solution with adding solution of K_2CrO_4 in ambient conditions.

Near-Infrared Luminescence

As depicted in Fig. 9, upon excitation maximum at 457 nm, the Nd(III) polymer **2** exhibits typical emission bands of Nd(III) ions in solid state, whereas the emission band from the free H_3ddpp ligand is not observed, indicating energy transfer from the ligand to Nd(III) center during photoluminescence process. The emission bands were observed at 920, 1054 and 1322 nm in near-infrared range, and they are attributed to the transitions from $^4F_{3/2}$ level to the $^4F_{3/2}\rightarrow{}^4I_{9/2}$, $^4F_{3/2}\rightarrow{}^4I_{13/2}$ and $^2F_{3/2}\rightarrow{}^4I_{15/2}$ sublevels of Nd(III), respectively.[41] It is well-known the neodymium(III) complex systems with an output wavelength around 1060 nm are of great interest for their potential application as liquid laser in high-power and high average-power outputs laser systems to overcome the inevitable heat accumulation problems of solid laser.[42] For the Er(III) polymer, as shown in Fig.10, under visible excitation at 462 nm the emission maximum is located at 1537 nm was observed. This is corresponding to the $^4I_{13/2} \rightarrow {}^4I_{15/2}$ transition. Emission was observed for DMF, ethanol, water, solvents with all near-IR-emitting ion in similar profile, except for Er(III), whose emission is not observed in water but is in dimethylsulfoxide (DMSO). This is due to the fact that water has strong absorption bands located in the 1500 nm region of the spectrum. Polymer **6** also displays emission bands at 887, 929, 1053 and 1186 nm, which correspond to the $^4F_{3/2} \rightarrow {}^4F_J$ (J = 9/2, 11/2, 13/2) transitions of Er(III) ion, resectively.[43]

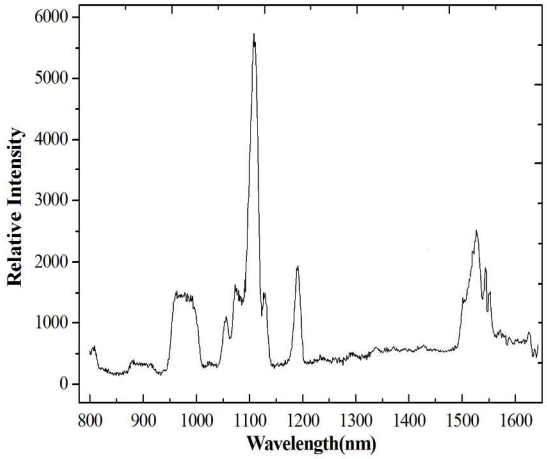

Fig. 9 The solid photo emission spectra of the compound **2** (Nd) under the visible region excitation at room temperature.

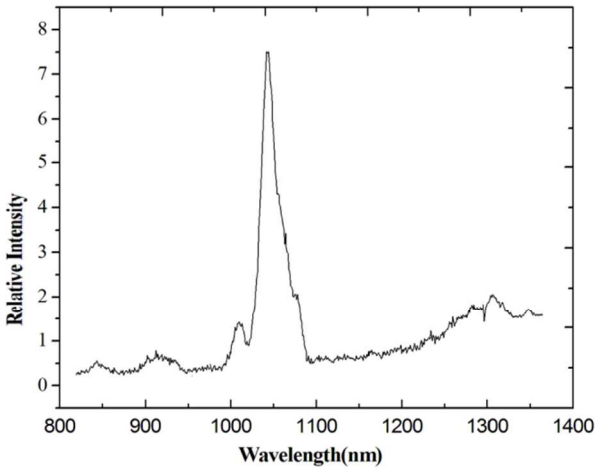

Fig. 10. Room temperature emission spectra for Er(III) polymer

6 in DMSO under the visible excitation in ambient conditions.

Conclusions

A series of new homonuclear lanthanide coordination polymers containing conjugated luminescent H_3ddpp ligand have been obtained. The LnCPs **1-6** exhibit crystal structures, dimensions and topologies diversities from light to heavy lanthanide cations with the lanthanide contraction phenomena. The H_3dppd ligand follows three different coordination models. Polymers **3** and **5** displayed the strong bright red and green luminescence due to the $4f^n$-$4f^n$ transitions in Eu(III) and Tb (III) ions, respectively. The potential luminescence sensing properties of polymer **5** indicates it is a luminescent sensory material for pollutant inorganic molecules. Polymers **2** and **6** can be excited in the visible region, and give strong NIR emissions that peak maximum at 1054 and 1536 nm, respectively.

Acknowledgements

This work was supported by the Natural Science Foundation of China (Nos. 51272231, 21273101 and 21271098). Foundation for Science & Technology Innovation Talents and Research Team in university of Henan (Nos. 2014HASTIT014 and 14IRTSTHN008), Tackle Key Problem of Science and Technology Project of Henan Province, (No.142102310483) and Ministry of Science and Technology of China (973 Project No. 2014CB660804). Science program from University of Malaya. (No. UM.C /625/1/HIR/247).

Notes and references

a. *College of Chemistry and Chemical Engineering, Luoyang Normal University, Luoyang, 471022, P. R. China. E-mail: fengx@lynu.edu.cn , wlya@lynu.edu.cn*

b. College of Chemistry and Pharmacy Engineering, Nanyang Normal University, Nanyang, 473601, P. R. China.

c. *Department of chemistry, University of Malaya, Kuala Lumpur, 50603, Malaysia.*

d Chemistry Department, Faculty of Science, King Abdulaziz University, Jeddah, 80203 Saudi Arabia

†Electronic Supplementary Information (ESI) available: X-Ray crystallographic files in CIF format (CCDC reference numbers 1412701-1412706). The additional structural, XRD patterns, luminescent and magnetic properties, figures and the selected bond distances and angles table, etc. See http://dx.doi.org/ 10.1039/b000000x/

1 (*a*) S. V. Eliseeva and J. C. G. Bünzli. *Chem. Soc. Rev.*, 2010, **39**, 189; (*b*) M. Gustafsson, A. Bartoszewicz, B. Mart′ın-Matute, J. Sun, J. Grins, T. Zhao, Z. Li, G. Zhu and X. Zou. *Chem. Mater.*, 2010, **22**, 3316; (*c*) J. W. Han and C. L. Hill. *J. Am. Chem. Soc.*, 2007, **129**, 15094; (*d*) N. Sabbatini, M. Guardigli, J. M. Lehn. *Coord. Chem. Rev*, 1993,**123**, 201.

2 (a) I. Hemmila. *J. Alloys. Compd*, 1995, **225**, 480; (b) J. Moynagh, H. Schimmel. *Nature*, 1999, **400**, 105; (c) F. S. Delgado, N. Kerbellec, C. Ruiz-Pérez, J. Cano, F. Lloret, M. Julve.*Inorg. Chem*. 2006, **45**, 1012.

3 S. I. Klink, H. Keizer and F. C. J. M. van Veggle. *Angew. Chem., Int. Ed*., 2000, **39**, 4319.

4 (*a*) J. Xu, J. W. Cheng, W. P. Su and M. C. Hong. *Cryst. Growth Des*., 2011, **11,** 2294; (*b*) G. Castro, R. Bastida, A. Macías, P. Pérez-Lourido, C. Platas-Iglesias, and L. Valencia. *Inorg. Chem*., 2015, **54,** 1671; (c) Z. He, E. Q. Gao, Z. M. Wang, C. H. Yan and M. Kurmoo. *Inorg. Chem.*, 2005, **44**, 862; (*d*) M. B. Zhang, J. Zhang, S. T. Zheng and G. Y. Yang. *Angew. Chem., Int. Ed.*, 2005, **44**, 1385; (*e*) X. J. Kong, Y. Wu, L. S. Long, L S. Zheng and Z. Zheng. *J. Am. Chem. Soc.*, 2009, **131**, 6918; (*f*) L. Cañadillas-Delgado, J. Pasán, O. Fabelo,M. Hernández-Molina, F. Lloret, M. Julve and C. Ruiz-Pérez, *Inorg. Chem*., 2006, **45**, 10585.

5 (*a*) B. V. Harbuzaru, A. Corma, F. Rey, J. L. Jord′a, D. Ananias, L. D. Carlos and J. Rocha. *Angew. Chem., Int. Ed.*,2009,**48**, 6476; (*b*) M. D. Allendorf, C. A. Bauer, R. K. Bhaktaa and R. J. T. Houka, *Chem. Soc. Rev.*, 2009,**38**, 1330; (*c*) B. Chen, Y. Yang, F. Zapata, G. Lin, G. Qian and E. B. Lobkovsky. *Adv. Mater*., 2007, **19,** 1693.

6 (*a*) Z. H. Zhang, Y. Song, T. Okamura, Y. Hasegawa, W. Y. Sun, N. Ueyama. *Inorg. Chem*., 2006, **45,** 2896; (*b*) J. Xia, B. Zhao, H. S. Wang, W. Shi, Y. Ma, H. B. Song, P. Cheng.*Inorg. Chem*., 2007, **46**, 3450.

7 (*a*) R. Cao, D. F. Sun, Y. C. Liang, M. C. Hong, K. Tatsumi and Q. Shi. *Inorg. Chem.*,2002, **41** , 2087; (*b*) D. Ghoshal, T. K. Maji, G. Mostafa, S. Sain, T. H. Lu, J. Ribas, E. Zangrando, N. R. Chaudhuri. *J. Chem. Soc. Dalton. Trans*., 2004, 1687; (*c*) S. N. Wang, H. Xing, J. F. Bai, Y. Z Li, Y. Pan, M. Scheer, X. Z. You. *Chem. Commun*., 2007, 2293; (*d*) B. Cheng Wang, Q. R. Wu, H.M. Hu, X.L.Chen, Z. H. Yang, Y. Q. Shangguan, M. L. Yang and G. L. Xue, *CrystEngComm*, 2010, **12**, 485; (*e*) S. N. Wang, H. Xing, J. F. Bai, Y. Z. Li, Y. Pan, M. Scheer, X. Z. You. *Cryst.Growth Des.*2007, **7**,747; (*f*) C. D. Wu, H. L. Ngo and W. Lin. *Chem. Commun.*, **2004**, 1588.

8 P. F. Shi, B. Zhao, G. Xiong, Y. L. Hou and P. Cheng. *Chem. Commun.*, 2012, **48**, 8231.

9 L. X. You, S. J. Wang, G. X., F. Ding, K. W. Meert, D. Poelman,P. F. Smet,B. Y. Ren, Y .W. Tian, and Y. G. Sun. *Dalton Trans.,* 2014, **43**, 17385.

10 X. Feng, J. S. Zhao, B. Liu, L. Y. Wang, J. G. Wang, S. W. Ng, G. Zhang, X. G. Shi , Y. Y. Liu. *Cryst. Growth Des.*2010, **10**, 1399.

11 (*a*) G. M. Sheldrick, SHELXS 97, *Program for the Solution of Crystal Structure*, University of Göttingen, Germany1997; (*b*) G. M. Sheldrick, SHELXL 97, *Program for the Crystal StructureRefinement*, University of Göttingen, Germany 1997**.**

12 K. Nakamoto, *Infrared and Raman Spectra of Inorganic and Coordination Compounds*, 4rded. Interscience-Wiley, New York, 1986.

13 X. Feng, B. Liu, L. Y. Wang, J. S. Zhao, J. G. Wang, S. W. Ng and X. G. Shi. *Dalton Trans.*, 2010, **39**, 8038.

14 (*a*) B. Gao, Q. Zhang, P. F. Yan, G. F. Hou and G. M. Li. *CrystEngComm*, 2013, **15**, 4167; (*b*) C. Hennig, A. Ikeda-Ohno, W. Kraus, S. Weiss, P. Pattison, H. Emerich, P. M. Abdala, and A. C. Scheinost. *Inorg. Chem*. 2013, **52**, 11734.

15 O. Delgado-Friedrichs, M. O'Keeffe. *ActaCrystallogr. A*, 2003, **59**, 351.

16 M. O'Keeffe, M. A. Peskov, S. J. Ramsden, O. M. Yaghi. *Acc. Chem. Res.*, 2008, **41**, 1782.

17 V. A. Blatov, M. O'Keeffe, D. M. Proserpio. *CrystEngComm*, 2010, **12**, 44.

18 E. V. Alexandrov, V. A. Blatov, A. V. Kochetkov, D. M. Proserpio. *CrystEngComm*, 2011, **13**, 3947.

19 (a) J. Jin, S. Y. Niu, Q. Han and Y. X. Chi. *New J. Chem.* 2010**, 34,** 1176; (b) M. Ahmad, R. Das, P. Lama, P. Poddar and P. K. Bharadwaj. *Crystal Growth Des.,* 2012, **12**, 4624; (c) S. S. Chen, Y. Zhao, J. Fan, T. Okamura, Z. S. Bai, Z. H. Chen and W. Y. Sun. *CrystEngComm.,*2012, **14,** 3564; (d) Y. Gong, J. H. Li, T. Wu, J. B. Qin, R. Cao and J. Li. *CrystEngComm.,*2012, **14,** 663; (e) J. J. Yang, L. Li, T. Yang, D. B. Kuang, W. Wang and C. Y. Su. *Chem.Commun.,* 2009**,** 17, 2387.

20 X. Feng, J. L. Cheng, L.Y. Wang, S. Y. Xie, S. Yang, S. Z. Huo and S. W. Ng. *CrystEngComm*, 2014, **16**, 1334.

21 T. Kundu, A. K. Jana, and S. Natarajan. *Cryst. Growth Des*, 2014, **14**, 4531.

22 (a) S. Petit,F. B. Robert, G. Pilet,C. Reberand D. Luneau. *Dalton Trans.*, 2009, 6809; (b) H. C. Liu, .H. Chen, A. Huang, S. C. Huang and K. F. Hsu. *Dalton Trans.*, 2009, 3447.

23 Z. Yan, M. Li, H. L. Gao, X. C. Huang, D. Li. *Chem. Commun.*, 2012, **48**, 3960.

24 J. Xiao, Y. Wu, M. Li, B. Y. Liu, X. C. Huang, D. Li. *Chem. Eur. J.*, 2013, **19**, 1891.

25 H. L. Zhou, M. Li, D. Li, J. P. Zhang, X. M. Chen. *Sci. China Chem.*, 2014, **57**, 365.

26 (*a*) A. Fratini, G. Richards, E. Larder and S. S wavey. *Inorg. Chem.*, 2008, **47**, 1030; (b) A. Fratini, S. Swavey. *Inorg. Chem.Commun*., 2007, **10**, 636; (*b*) Z. H. Zhang, T. A. Okamura, Y. Hasegawa, H. Kawaguchi,L. Y. Kong, W. Y. Sun and N. Ueyama. *Inorg. Chem*., 2005, **44**, 6219.

27 Y. M. Issa, H. M. Abdel Fattah, A. A. Soliman. *J. Thermal Anal.* 1994**, 42,** 1175.

28 (*a*)T. H. Zhou, F. Y. Yi, P. X. Li and J. G. Mao, *Inorg. Chem*., 2010, **49,** 905; (*b*) T. Kajiwara, M. Hasegawa, A. Ishii, K. Katagiri, M. Baatar, S. Takaishi, N. Iki, M. Yamashita. *Eur. J. Inorg. Chem*. 2008, **36**, 5565; (*c*) J. P. Costes, J. M. Clemente, Juan, F. Dahan, F. Nicodēme. *Dalton Trans*., 2003, 1272.

29 C. M. Wang, Y. Y. Wu, Y. W. Chang, and K. H. Li, *Chem. Mater.* 2008, **20***,* 2857.

30 (*a*) J. C. G. Bunzli, *Lanthanide Probes in Life, Chemical, and Earth Sciences: Theory and Practice*, Elsevier Science Publications: Amsterdam, **1989**; (*b*) Evan G. Moore, Amanda P. S. Samuel and Kenneth N. Raymond, *Acc. Chem. Res.*, 2009,***42*** (4), 542.

31 X. Feng, Y. Q. Feng,J. J. Chen, S. W. Ng, L. Y. Wang, J. Z. Guo. *Dalton Trans.,* 2015, **44,** 804.

32 (*a*) P. A. Brayshaw, J. C. G. Bunzli, P. Froidevaux, J. M. Harrowfield, Y. Kim, A. N. Sobolev. *Inorg. Chem*. 1995, **34**, 2068; (*b*) W. S. Lo, J.H. Zhang, W. T. Wong, and G. L. Law. *Inorg. Chem.*, 2015, **54**, 3725.

33 A. Y. Robin, K. M. Fromm. *Coord. Chem. Rev*. 2006, **250**, 2127.

34 D. B. A. Raj, B. Francis, M. L. P. Reddy, R. R. Butorac, V. M. Lynch and A. H. Cowley. *Inorg. Chem.*, 2010, **49**, 9055.

35 S. Osa, T. Kido, N. Matsumoto, N. Re, A. Pochaba, J. Mrozinski. *J. Am. Chem. Soc*., 2004, **126**, 420.

36 J. Claude, G. Bünzli. *Chem. Rev.,* 2010,**110**, 2729.

37 (a) P. A. Tanner, *Chem. Soc. Rev.* 2013, **42**, 5090. (b) S. Quici, G. Marzanni, M. Cavazzini, P. L. Anelli, M. Botta, E. Gianolio, G. Accorsi, N. Armaroli, F. Barigelletti. *Inorg. Chem.* 2002, *41*, 2777.

38 (a) B. D. Chandler, J. O. Yu , David T. Cramb and George K. H. Shimizu. *Chem. Mater.*, 2007, ***19***, 4467; (b) R. A. Poole, G. C. Bobba, M. J. Frias, J. C. Parker, D. Peacock, R. D. Org. *Biomol. Chem.*2005, **3**, 1013; (c) A. P. S. Samuel, E. G. Moore, M. Melchior, J. Xu, K. N. Raymond. *Inorg. Chem.* 2008, **47,** 7535; (d) A.S. Chauvin, F. Gumy, D. Imbert, J. C. G. Bünzli. *Spectrosc. Lett.* 2004, **37**, 517.

39 (a) S. Faulkner and S. J. A. Pope. *J. Am. Chem. Soc.*, 2003, ***125***, 10526; (b) S. Quici, M. Cavazzini, G. Marzanni, G. Accorsi, N. Armaroli, B. Ventura, and F. Barigelletti. *Inorganic Chemistry,* 2005, **44**, 529; (c) X. Q. Song, Y. K. Lei, X. R. Wang, M. M. Zhao, Y. Q. Peng, G. Q. Cheng. *J Solid State Chem.*2014, ***218***, 202.

40 (a)B. D. Anade, P. S. Barber, and S. Bauer. *J. Am. Chem. Soc.* 2012, **134**, 6987; (b) Q. Tang, S. X. Liu, Y. W. Liu, D. F. He, J. Miao, Y. J. Ji and Z. P. Zheng, *Inorg. Chem.* 2014, **53**, 289.

41 (a) J –G. Lin, Y.Y. Xu, L. Qiu, S-Q. Zang, C. S. Lu, C-Y. Duan, Y. Z .Li, S. Gao and Q. J. Meng, *Chem. Commun*., 2008, 2659; (b) B. L. Chen, L. B. Wang, F. Zapata, G. D. Qian and E. B. Lobkovsky. *J. Am. Chem. Soc.*, 2008, **130**, 6718; (c) S. Comby, S. A. Tuck, L. K. Truman, O. Kotova, and T. Gunnlaugsson. *Inorg. Chem.* 2012, **51**, 10158.

42 (a) X. Qiu, K. Yu, C. Gao, C. Hou, J. He, Z. Zhou, W. Wei, B. Peng, *Chem. Phys. Lett*, 2008, **457**, 194; (b) J. Lu, K Yu., H. Wang, J. He, G .Cheng, C. Qin, J. Lin, W. Wei, B. Peng, *Opt. Mater*, 2008, **30**, 1531; (*c*) X. Feng, J. G. Wang, B. Liu, L. Y. Wang, J. S.Zhao, S. W. Ng. *Cryst. Growth Des*. 2012, **12**, 927.

43 (a) J. Zhang and S. Petoud. *Chem. Eur. J.* 2008, **14**, 1264;(b) P. Abrice, L. G. Boris, C. Thomas, G. Stéphane, C. Olivier, M. Oliviervand O. Lahcène, *Inorg. Chem*. 2013, **52**, 5978.

Series of homonuclear lanthanide–coordination polymers incorporating conjugated ligand of 2,5-di(2',4'-dicarboxylpheny) pyridine have been fabricated successfully, and characterized systematically.